arXiv:1507.03700v1 [hep-ph] 14 Jul 2015

OUTP-15-15P
TUM-HEP-1005/15
SI-HEP-2015-17
QFET-2015-23
July 13, 2015

Two-loop current-current operator contribution to the non-leptonic QCD penguin amplitude

G. Bell[a], M. Beneke[b], T. Huber[c] and Xin-Qiang Li[d,e]

[a] *Rudolf Peierls Centre for Theoretical Physics, University of Oxford, 1 Keble Road, Oxford OX1 3NP, United Kingdom*

[b] *Physik Department T31, Technische Universität München, James-Franck-Straße 1, D-85748 Garching, Germany*

[c] *Theoretische Physik 1, Naturwissenschaftlich-Technische Fakultät, Universität Siegen, Walter-Flex-Strasse 3, D-57068 Siegen, Germany*

[d] *Institute of Particle Physics and Key Laboratory of Quark and Lepton Physics (MOE), Central China Normal University, Wuhan, Hubei 430079, P. R. China*

[e] *State Key Laboratory of Theoretical Physics, Institute of Theoretical Physics, Chinese Academy of Sciences, Beijing 100190, P. R. China*

Abstract

The computation of direct CP asymmetries in charmless B decays at next-to-next-to-leading order (NNLO) in QCD is of interest to ascertain the short-distance contribution. Here we compute the two-loop penguin contractions of the current-current operators $Q_{1,2}$ and provide a first estimate of NNLO CP asymmetries in penguin-dominated $b \to s$ transitions.

1 Introduction

Non-leptonic exclusive decays of B mesons play a crucial role in studying the CKM mechanism of quark flavour mixing and in quantifying the phenomenon of CP violation. Direct CP violation is related to the rate difference of $\bar{B} \to f$ decay and its CP-conjugate and arises if the decay amplitude is composed of at least two partial amplitudes with different re-scattering ("strong") phases, which are multiplied by different CKM matrix elements. Very often useful information on the CKM parameters including the CP-violating phase can be obtained from combining different decay modes, whose partial amplitudes are related by the approximate flavour symmetries of the strong interaction [1], which are then determined from data.

The direct computation of the partial amplitudes is a complicated strong interaction problem, which can, however, be addressed in the heavy-quark limit. The QCD factorization approach [2–4] employs soft-collinear factorization in this limit to express the hadronic matrix elements in terms of form factors and convolutions of perturbative objects (hard-scattering kernels) with non-perturbative light-cone distribution amplitudes (LCDAs). At leading order in Λ/m_b,

$$\begin{aligned}\langle M_1 M_2 | Q_i | \bar{B} \rangle \;=\; & i m_B^2 \left\{ f_+^{BM_1}(0) \int_0^1 du \; T_i^I(u) \, f_{M_2} \phi_{M_2}(u) + (M_1 \leftrightarrow M_2) \right. \\ & \left. + \int_0^\infty d\omega \int_0^1 du dv \; T_i^{II}(\omega, v, u) \, \hat{f}_B \phi_B(\omega) \; f_{M_1} \phi_{M_1}(v) \; f_{M_2} \phi_{M_2}(u) \right\}, \qquad (1)\end{aligned}$$

where Q_i is a generic operator from the effective weak Hamiltonian. At this order the re-scattering phases are generated at the scale m_b only, and reside in the loop corrections to the hard-scattering kernels. Beyond the leading order factorization does not hold, and re-scattering occurs at all scales. The leading contributions to the strong phases are therefore of order $\alpha_s(m_b)$ or/and Λ/m_b. It is of paramount importance for the predictivity of the approach for the direct CP asymmetries to know whether the short-distance or long-distance contribution dominates in practice, since apart from being parametrically small, both could be numerically of similar size.

The short-distance contribution to the direct CP asymmetries is fully known only to the first non-vanishing order (that is, $\mathcal{O}(\alpha_s)$) through the one-loop computations of the vertex kernels T_i^I performed long ago [2, 4, 5]. A reliable result presumably requires the next-to-next-to-leading order $\mathcal{O}(\alpha_s^2)$ hard-scattering kernels, at least their imaginary parts. For the spectator-scattering kernels T_i^{II} this task is already completed, both for the tree [6–8] and penguin [9, 10] amplitudes, but for the so-called form factor term(s) in the first line of (1) an important piece is still missing, which is the focus of this Letter.

We recall that due to CKM unitarity, the amplitude for a $\bar{B}$ decay governed by the $b \to D$ ($D = d, s$) transition can always be written in the form

$$A(\bar{B} \to f) = \lambda_u^{(D)} \, [T + \ldots] + \lambda_c^{(D)} \, [P_c + \ldots], \qquad (2)$$

where $\lambda_p^{(D)} = V_{pD}^* V_{pb}$. It is generic that the first CKM structure is dominated by the colour-allowed or colour-suppressed topological tree amplitude, both denoted by T here, corresponding to the flavour quantum numbers of a $b \to u\bar{u}D$ transition, while the second is dominated by the topological QCD penguin amplitude of the $b \to \sum_{q=u,d,s} q\bar{q}D$ transition. The first is typically larger than the second for $D = d$ and vice-versa for the $D = s$ case, which therefore refers to the penguin-dominated decays such as $\bar{B} \to \pi K$ and related. In the notation of [5, 9], P_c corresponds to the quantity $\alpha_4^c(M_1M_2)$.[1]

The vertex kernels T_i^I have been computed at the two-loop $\mathcal{O}(\alpha_s^2)$ order only for the topological tree amplitudes T [11–13]. However, direct CP asymmetries can only be non-zero due to the interference of the two terms in (2), hence the penguin amplitude P_c is also needed. Only the one-loop $\mathcal{O}(\alpha_s^2)$ contribution from the chromomagnetic dipole operator Q_{8g} to P_c has been considered in the past [14], while the dominant, genuine two-loop contributions remain to be computed. This calculation is technically very involved since it requires the computation of massive two-loop penguin diagrams – a genuine two-loop, two-scale problem. One step towards this goal was recently achieved in [15], where analytic results of all occurring master integrals were derived.

At this point it is important to note that the topological tree and penguin amplitudes are not in one-to-one correspondence with the tree (or current-current) operators $Q_{1,2}^p$ and QCD penguin operators Q_{3-6} of the weak effective Hamiltonian. By contracting the $p\bar{p}$ fields of the operators $Q_{1,2}^p$ (see (5) below), they contribute to the QCD penguin amplitude starting from the one-loop order. Since these "penguin contractions" of the current-current operators come with the large short-distance coefficients $C_{1,2}$, we may argue that they constitute the largest contribution to the penguin amplitude at any given loop order.[2] At *next-to-leading order* we find for the penguin contractions (including the chromomagnetic dipole operator Q_{8g})

$$\begin{aligned} a_4^u(\pi\bar{K})_{|\text{NLO}} &= (-0.0087 - 0.0172i)_{|Q_{1,2}} + (0.0042 + 0.0041i)_{|Q_{3-6}} + 0.0083_{|Q_{8g}}, \\ a_4^c(\pi\bar{K})_{|\text{NLO}} &= (-0.0131 - 0.0102i)_{|Q_{1,2}} + (0.0042 + 0.0041i)_{|Q_{3-6}} + 0.0083_{|Q_{8g}}, \end{aligned} \tag{3}$$

where we separated the contributions from the current-current and the other operators. While there is a cancellation for the real part, the imaginary part from $Q_{1,2}^p$ is clearly dominant. If we add the vertex contractions at leading (LO) and next-to-leading order (NLO) and consider the entire form factor contribution to $a_4^p(M_1M_2)$ at NLO, the second term changes to $(-0.0266 + 0.0032i)_{|Q_{3-6}}$ in both expressions, and the imaginary part from $Q_{1,2}^p$ is still by far dominant. Thus, at NLO, the short-distance direct CP asymmetries are mainly determined by the one-loop penguin contractions of the current-current operators. It is reasonable to assume that the insertion of $Q_{1,2}^{u,c}$ at two loops also captures the bulk of the yet unknown NNLO form factor contribution T_i^I to the penguin amplitudes $a_4^{u,c}$. In this Letter we report the result of this computation together with

---

[1] $\alpha_4^u(M_1M_2)$ refers to a generically sub-leading penguin contribution to the term multiplied by the CKM factor $\lambda_u^{(D)}$. We also note that $\alpha_4^p(M_1M_2)$ consists of a leading-power term a_4^p and a power-suppressed term a_6^p [5]. The calculation reported here concerns the leading-power contribution a_4^p.

[2] Since the contribution from $Q_{1,2}^p$ alone is not renormalization-group invariant, this statement cannot be true in arbitrary schemes nor at arbitrary renormalization scales. What we mean is that the statement holds in the conventional $\overline{\text{MS}}$ scheme and with a reasonable choice $\mathcal{O}(m_b)$ of scale.

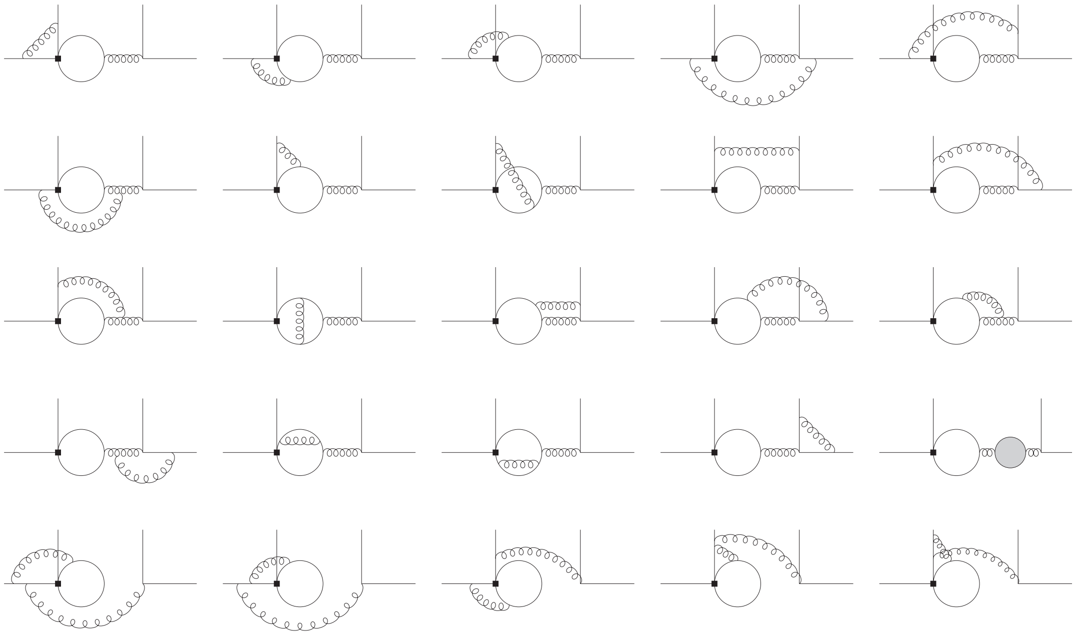

Figure 1: Two-loop penguin diagrams that contribute to the insertion of the operators $Q^{u,c}_{1,2}$ (black square). The grey filled circle denotes the one-loop gluon self-energy.

a few phenomenological implications. We shall provide more technical details together with the remaining contributions from the QCD penguin operators Q_{3-6}, which require additional work on infrared subtractions not present for $Q^p_{1,2}$, in a future publication.

2 Outline of the calculation

The effective weak Hamiltonian for $b \to D$ transitions ($D = d, s$) is given by

$$\mathcal{H}_{\text{eff}} = \frac{4G_F}{\sqrt{2}} \sum_{p=u,c} V^*_{pD} V_{pb} \bigg(C_1 Q^p_1 + C_2 Q^p_2 + \ldots \bigg) + \text{h.c.}. \tag{4}$$

Here and in the following we give explicitly only the definitions pertinent to the current-current operators relevant to our calculation. We adopt the Chetyrkin-Misiak-Münz (CMM) operator basis [16], where the current-current operators are defined as

$$Q^p_1 = (\bar{p}_L \gamma^\mu T^A b_L)\,(\bar{D}_L \gamma_\mu T^A p_L), \qquad Q^p_2 = (\bar{p}_L \gamma^\mu b_L)\,(\bar{D}_L \gamma_\mu p_L), \tag{5}$$

in terms of left-chiral quark fields $q_L = \frac{1}{2}(1-\gamma_5)q$. In dimensional regularization the operator basis has to be supplemented by evanescent (vanishing in $D = 4$ dimensions) operators, for which we adopt the convention of [17].

At the two-loop level about 70 diagrams contribute to the QCD penguin amplitude, but only a subset of two dozens (shown in Fig. 1) are non-vanishing for the insertion of the current-current operators $Q^p_{1,2}$. The quark in the fermion loop can either be massless (for $p = u$) or massive (for $p = c$). In the massless case the problem involves one non-trivial scale, the momentum fraction $\bar{u} = 1 - u$ of the anti-quark in meson M_2, and the structure is similar to the NNLO calculation of the tree amplitudes [11–13]. In the massive case, however, we are dealing with a genuine two-loop, two-scale problem since the hard-scattering kernels depend in addition on the mass ratio $s_c = m_c^2/m_b^2$. As we have already elaborated extensively on the kinematics in [15], we shall not repeat those formulae here.

The calculation is performed in dimensional regularization with $D = 4 - 2\epsilon$, where ultraviolet (UV) and infrared (soft and collinear) divergences manifest themselves as poles in ϵ. The CMM basis ensures that the NDR scheme with a fully anti-commuting γ_5 can be adopted. The amplitude of the diagrams is then computed using standard multi-loop techniques. After a Passarino-Veltman [18] decomposition of the tensor integrals, the scalar integrals are reduced to a small set of master integrals by means of integration-by-parts techniques [19, 20] and the Laporta algorithm [21, 22]. To this end, we use the program AIR [23] as well as an in-house routine.

For the massless up-type operator insertions, the diagrams can be expressed in terms of the master integrals that appeared in our former calculations [11–13]. For the massive charm-type insertions, on the other hand, we find 29 new master integrals. The computation of the master integrals constitutes the main technical challenge of the calculation. Analytic results for all master integrals have recently been derived in [15], based on a differential equation approach in a canonical basis [24]. The canonical basis, together with suitably chosen kinematic variables, also catalyses the convolution of the hard-scattering kernels with the LCDA.

After the computation of the bare QCD two-loop amplitude, the hard-scattering kernels are extracted from a matching calculation onto soft-collinear effective theory (SCET). The main conceptual challenge in this context is the consistent treatment of evanescent and Fierz-equivalent operators in SCET, for which we follow the method employed in [13]. The SCET operators have the flavour structure $\sum_q (\bar{\chi}_D \chi_q)(\bar{\xi}_q h_v)$ where χ and ξ denote collinear light-quark fields moving in opposite directions. The two-loop diagrams relevant to the penguin amplitude a_4^p are all of the "wrong-insertion" type (see [13]) and hence lead to operators where the fermion indices are contracted in the form $\sum_q (\bar{\xi}_q \chi_q)(\bar{\chi}_D h_v)$. In Fig. 1 the $(\bar{\xi}_q \chi_q)$ fermion lines correspond to the solid line on the right side of the diagram. In the following we omit the sum over q and the flavour labels on the fields. In the CMM basis the fermion line that corresponds to $(\bar{\xi}\chi)$ carries no γ_5 matrix. This suggests that we use the following basis for the SCET operators:

$$\begin{aligned} O_1 &= \bar{\chi}\,\frac{\not{n}_-}{2}(1-\gamma_5)\chi\,\bar{\xi}\,\not{n}_+(1-\gamma_5)h_v\,, \\ \tilde{O}_n &= \bar{\xi}\,\gamma_\perp^\alpha \gamma_\perp^{\mu_1} \gamma_\perp^{\mu_2} \dots \gamma_\perp^{\mu_{2n-2}} \chi\,\bar{\chi}(1+\gamma_5)\gamma_{\perp\alpha}\gamma_{\perp\mu_{2n-2}}\gamma_{\perp\mu_{2n-3}} \dots \gamma_{\perp\mu_1} h_v, \end{aligned} \tag{6}$$

where we need n up to 2 (strings with three γ matrices in each bilinear). The operator O_1 is the only physical SCET operator. It is the same as in [13], whereas the $\tilde{O}_n$ differ by the absence of the $1 - \gamma_5$ factor to the left of χ. The operators $\tilde{O}_n$ are evanescent for $n > 1$. $\tilde{O}_1$ is Fierz-equivalent to $O_1/2$ in four dimensions, so we add $\tilde{O}_1 - O_1/2$ as another evanescent operator. We also recall that the SCET operators are non-local on the light-cone [13].

After operator matching the hard-scattering kernels follow from the bare QCD amplitudes plus subtraction terms from UV counterterms of the operators Q_i and the SCET operators. The master formulae at LO, NLO, and NNLO read, respectively,

$$\widetilde{T}_i^{(0)} = \widetilde{A}_{i1}^{(0)} \,, \tag{7}$$

$$\widetilde{T}_i^{(1)} = \widetilde{A}_{i1}^{(1)\mathrm{nf}} + Z_{ij}^{(1)}\, \widetilde{A}_{j1}^{(0)} + \ldots \,, \tag{8}$$

$$\begin{aligned}\widetilde{T}_i^{(2)} &= \widetilde{A}_{i1}^{(2)\mathrm{nf}} + Z_{ij}^{(1)}\, \widetilde{A}_{j1}^{(1)} + Z_{ij}^{(2)}\, \widetilde{A}_{j1}^{(0)} + Z_{\alpha}^{(1)}\, \widetilde{A}_{i1}^{(1)\mathrm{nf}} + (-i)\, \delta m^{(1)}\, \widetilde{A}_{i1}^{\prime(1)\mathrm{nf}} \\ &\quad + Z_{ext}^{(1)} \big[\widetilde{A}_{i1}^{(1)\mathrm{nf}} + Z_{ij}^{(1)}\, \widetilde{A}_{j1}^{(0)}\big] - \widetilde{T}_i^{(1)} \big[C_{FF}^{(1)} + \widetilde{Y}_{11}^{(1)}\big] + \ldots \,. \end{aligned} \tag{9}$$

The symbols have the same meaning as in Eq. (29) of [13]. The ellipses denote further terms that do not contribute to the kernels $i = 1, 2$ of the current-current operators. The matrices $Z_{ij}^{(1)}$ and $Z_{ij}^{(2)}$ contain the UV counterterms from operator mixing. Compared to the calculation of the tree amplitudes, they have to be extended by the mixing with the penguin operators including the correspondent evanescent operators [17]. This implies, in particular, that the one-loop amplitudes $\widetilde{A}_{j1}^{(1)}$ must be computed including the $\mathcal{O}(\epsilon)$ terms for all operators Q_j, which mix with the current-current operators. Finally, one has to convolute the hard-scattering kernels with the LCDA, for which we adopt the conventional Gegenbauer expansion.

3 The topological QCD penguin amplitude

In this section we give the numerical results of the penguin amplitudes a_4^u and a_4^c and discuss the size and scale dependence of the new contribution. At LO, the penguin amplitude coefficients are given in the CMM basis by ($N_c = 3$, $C_F = 4/3$)

$$a_{4,\mathrm{LO}}^p = \frac{1}{N_c} \left[C_3 + C_F C_4 + 16(C_5 + C_F C_6)\right]. \tag{10}$$

They are identical for $p = u, c$ and independent of the LCDA. At NLO we have ($L = \ln \mu^2/m_b^2$, $s_p = m_p^2/m_b^2$, $\bar{u} = 1 - u$)

$$a_{4,\mathrm{NLO}}^p|_{C_{1,2}} = \frac{\alpha_s}{4\pi} \frac{C_F}{N_c} \left(C_2 - \frac{C_1}{2N_c}\right) \int_0^1 du \left[-\frac{2}{3}L + \frac{2}{3} - G(s_p - i\epsilon, \bar{u})\right] \phi_{M_2}(u), \tag{11}$$

where we show only the terms from the current-current operators to illustrate the structure of the result. Here

$$G(s,u) = \frac{2(12s + 5u - 3u \ln s)}{9u} - \frac{2\xi(2s+u)}{3u} \ln \frac{\xi+1}{\xi-1} \tag{12}$$

is the one-loop penguin function with $\xi = \sqrt{1 - 4s/u}$. In practice, one then inserts the Gegenbauer expansion of $\phi_{M_2}(u)$ truncated at the second order to perform the integral.

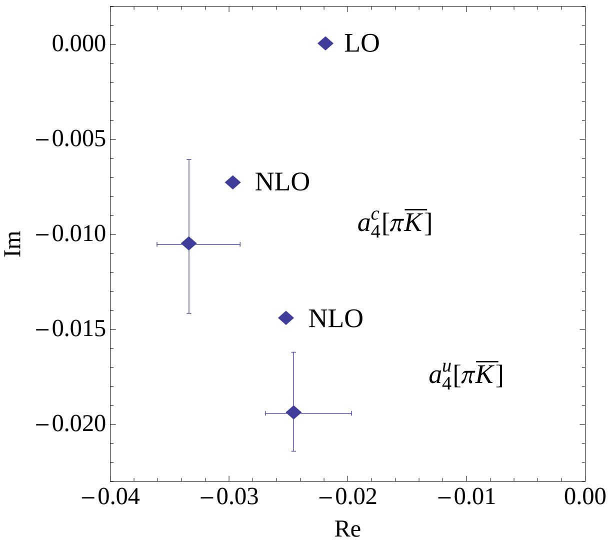

Figure 2: The LO, NLO and NNLO values of $a_4^u(\pi\bar{K})$ and $a_4^c(\pi\bar{K})$ in the complex plane. The NNLO point includes a theoretical error estimate.

The result is finally expressed in terms of Wilson coefficients, quark masses and the Gegenbauer moments $a_{1,2}^{M_2}$.

At NNLO the explicit expressions are involved, and we postpone the details to a future publication. Our final numerical predictions for the leading QCD penguin amplitudes $a_4^{u,c}(\pi\bar{K})$ are given as (for input parameters, see section 4):

$$\begin{aligned} a_4^u(\pi\bar{K})/10^{-2} &= -2.87 - [0.09+0.09i]_{\mathrm{V}_1} + [0.49-1.32i]_{\mathrm{P}_1} - [0.32+0.71i]_{\mathrm{P}_2} \\ &\quad + \left[\frac{r_{\mathrm{sp}}}{0.434}\right]\Big\{[0.13]_{\mathrm{LO}} + [0.14+0.12i]_{\mathrm{HV}} - [0.01-0.05i]_{\mathrm{HP}} + [0.07]_{\mathrm{tw3}}\Big\} \\ &= (-2.46^{+0.49}_{-0.24}) + (-1.94^{+0.32}_{-0.20})i\,, \end{aligned} \tag{13}$$

$$\begin{aligned} a_4^c(\pi\bar{K})/10^{-2} &= -2.87 - [0.09+0.09i]_{\mathrm{V}_1} + [0.05-0.62i]_{\mathrm{P}_1} - [0.77+0.50i]_{\mathrm{P}_2} \\ &\quad + \left[\frac{r_{\mathrm{sp}}}{0.434}\right]\Big\{[0.13]_{\mathrm{LO}} + [0.14+0.12i]_{\mathrm{HV}} + [0.01+0.03i]_{\mathrm{HP}} + [0.07]_{\mathrm{tw3}}\Big\} \\ &= (-3.34^{+0.43}_{-0.27}) + (-1.05^{+0.45}_{-0.36})i\,. \end{aligned} \tag{14}$$

In both equations the second line represents the spectator-scattering term, which for $r_{\mathrm{sp}} = 0.434$ makes only a small contribution to a_4^p. In the respective first lines, the number without brackets is the LO contribution, which has no imaginary part, the following two numbers are the vertex and penguin NLO terms, and the new two-loop NNLO contribution from the current-current operators $Q_{1,2}^p$ is the number labelled P_2. We observe that the new correction is rather large. It amounts approximately to 40% (15%) of the imaginary (real) part of $a_4^u(\pi\bar{K})$, and 50% (25%) in the case of $a_4^c(\pi\bar{K})$. Graphical representations of $a_4^p(\pi\bar{K})$ are shown in Fig. 2 at LO, NLO and NNLO, where the NNLO

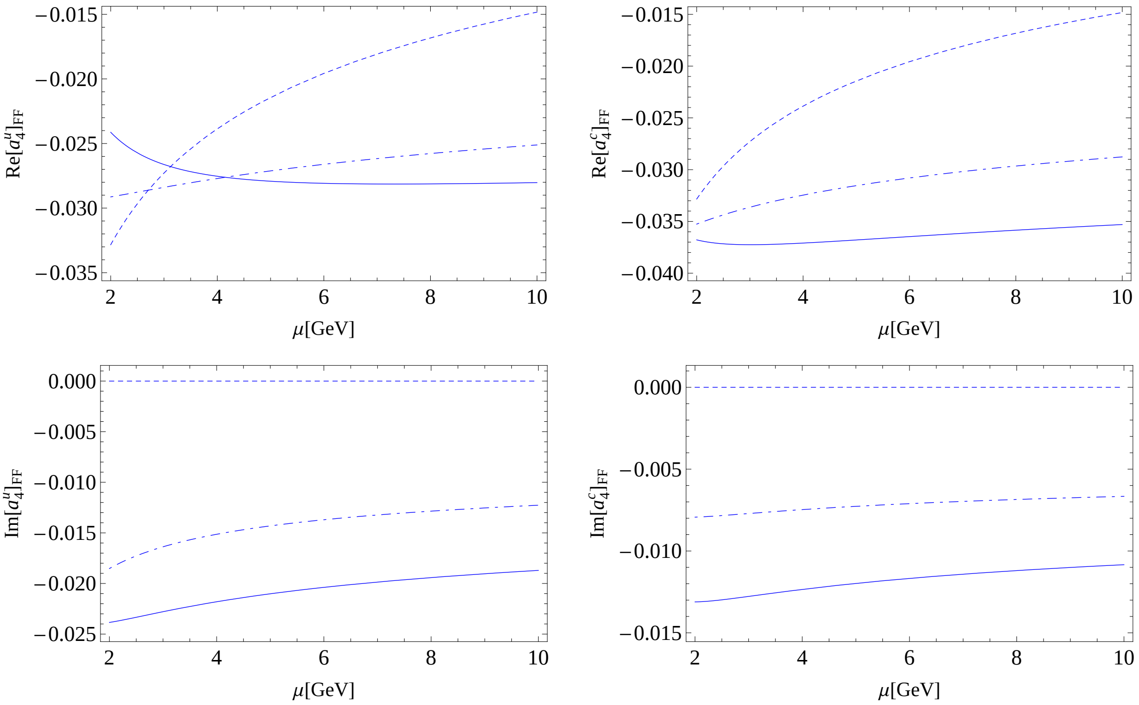

Figure 3: The dependence of the leading QCD penguin amplitudes $a_4^p(\pi\bar{K})$ on the hard renormalization scale μ (form factor term only). Dashed, dashed-dotted and solid lines represent LO, NLO, and NNLO, respectively.

point includes the theoretical error estimate.[3] The larger uncertainty of the imaginary part of $a_4^c(\pi\bar{K})$ is a consequence of the sensitivity to the charm-quark (pole) mass, for which we adopt the conservative range $m_c = 1.3 \pm 0.2\,\text{GeV}$.

The values (13), (14) depend on the renormalization scale due to the truncation of the perturbative expansion and on hadronic parameters. The dependence on the renormalization scale μ may be considered as a measure of the accuracy of the approximation at a given order in perturbation theory. This is shown in Fig. 3 for the form factor term contribution to $a_4^p(\pi\bar{K})$ up to NNLO. We observe a considerable stabilization of the scale dependence for the real part, but less for the imaginary part. This is explained by the fact that the imaginary part vanishes at LO. Hence only the first correction is now available and is, moreover, large.

4 Phenomenology – direct CP asymmetries

We now consider the new contribution to a_4^p in the context of the full QCD penguin amplitude and provide first results for some direct CP asymmetries. We defer the discussion of branching fractions to the more complete treatment including the two-loop matrix elements of the penguin operators Q_{3-6}.

---

[3] The LO and NLO numbers here as in the subsequent figure are not the same as (13), (14) truncated to LO and NLO, because they employ Wilson coefficients C_i at LO and NLO, respectively. Moreover, consistent with previous LO and NLO calculations, they are computed in the operator basis as defined in [25]. On the other hand, in (13), (14) NNLO Wilson coefficients in the CMM basis are used throughout.

We recall that in the QCD factorization approach the full QCD penguin amplitude consists of the parameters a_4^p, a_6^p, and the penguin annihilation amplitude β_3^p in the combination [5]

$$\hat{\alpha}_4^p(M_1M_2) = a_4^p(M_1M_2) \pm r_\chi^{M_2} a_6^p(M_1M_2) + \beta_3^p(M_1M_2), \tag{15}$$

where the plus (minus) sign applies to the decays where M_1 is a pseudoscalar (vector) meson. The first term, $a_4^p(M_1M_2)$, is the only leading-power contribution. Its real part is of order -0.03. The annihilation term is $1/m_b$ suppressed and cannot be calculated in the factorization framework. Estimates based on the model defined in [4] suggest that its modulus is also of order 0.03. While the magnitude of these two terms is largely independent of the spin of the final state mesons, the contribution from the power-suppressed scalar penguin amplitude $r_\chi^{M_2} a_6^p(M_1M_2)$ is very small when M_2 is a vector meson, but larger than the leading-power amplitude for pseudoscalar M_2. It interferes constructively for the PP final state, and destructively for VP. It follows from this brief discussion that the impact of a correction to a_4^p is always diluted in the full penguin amplitude. When $M_2 = V$, the computation of a_4^p ascertains the short-distance contribution to the amplitude, and hence the direct CP asymmetry, but there is an uncertain annihilation contribution of similar size. When $M_2 = P$, there is another NNLO short-distance contribution from a_6^p, which is difficult though not impossible to calculate, since it is power-suppressed. These features will be clearly seen in the analysis below.

In the following we adopt the same values for the Standard Model, meson and form factor parameters as in Table 1 of [13] with the exception of $|V_{ub}/V_{cb}| = 0.085 \pm 0.015$, $\tau_{B_d} = 1.52\,\mathrm{ps}$, $m_s(2\,\mathrm{GeV}) = (90 \pm 10)\,\mathrm{MeV}$, and $f_{B_d} = (190 \pm 10)\,\mathrm{MeV}$. The decay constants, Gegenbauer moments and form factors involving kaons coincide with [9], those involving K^* mesons with [5], except for $A_0^{BK^*}(0) = 0.39 \pm 0.06$. We note that the B-meson LCDA parameter λ_B is not important here, since the leading spectator-scattering contribution to the QCD penguin amplitude is colour-suppressed.

In Fig. 4 we show the QCD penguin amplitude $\hat{\alpha}_4^c(M_1M_2)$ normalized to the sum of colour-allowed and colour-suppressed tree amplitude $\alpha_1(\pi\pi) + \alpha_2(\pi\pi)$,[4] as was shown before in [5,9], but now includes the NNLO computation for numerator and denominator. The NNLO result is represented by the dark point with error bars and corresponds to setting $\varrho_A = 0$ in the annihilation model, which implies a small value of β_3^c. The nearly circular contours around this point show the variation of the theoretical prediction when the phase of the annihilation model is varied from 0 to 2π for fixed $\varrho_A = 1, 2, 3$ (inner to outer circles). The radius of the circle for $\varrho_A = 1$ leads to the estimate $|\beta_3^c| \approx 0.03$ mentioned above. The LO and NLO results are marked by diamonds without error bars. Despite the sizable NNLO correction to a_4^c as shown in Fig. 2, the difference between NNLO and NLO is small. This is a consequence of the "dilution" discussed above and a partial cancellation in the ratio of amplitudes.

---

[4] For $M_1M_2 = \pi\bar{K}$, $\pi\bar{K}^*$. For $M_1M_2 = \rho\bar{K}$, $\rho\bar{K}^*$ we use the $\rho\rho$ final state instead. Also, for $\rho\bar{K}^*$ and $\rho\rho$, only the longitudinal polarization amplitude is considered in the following.

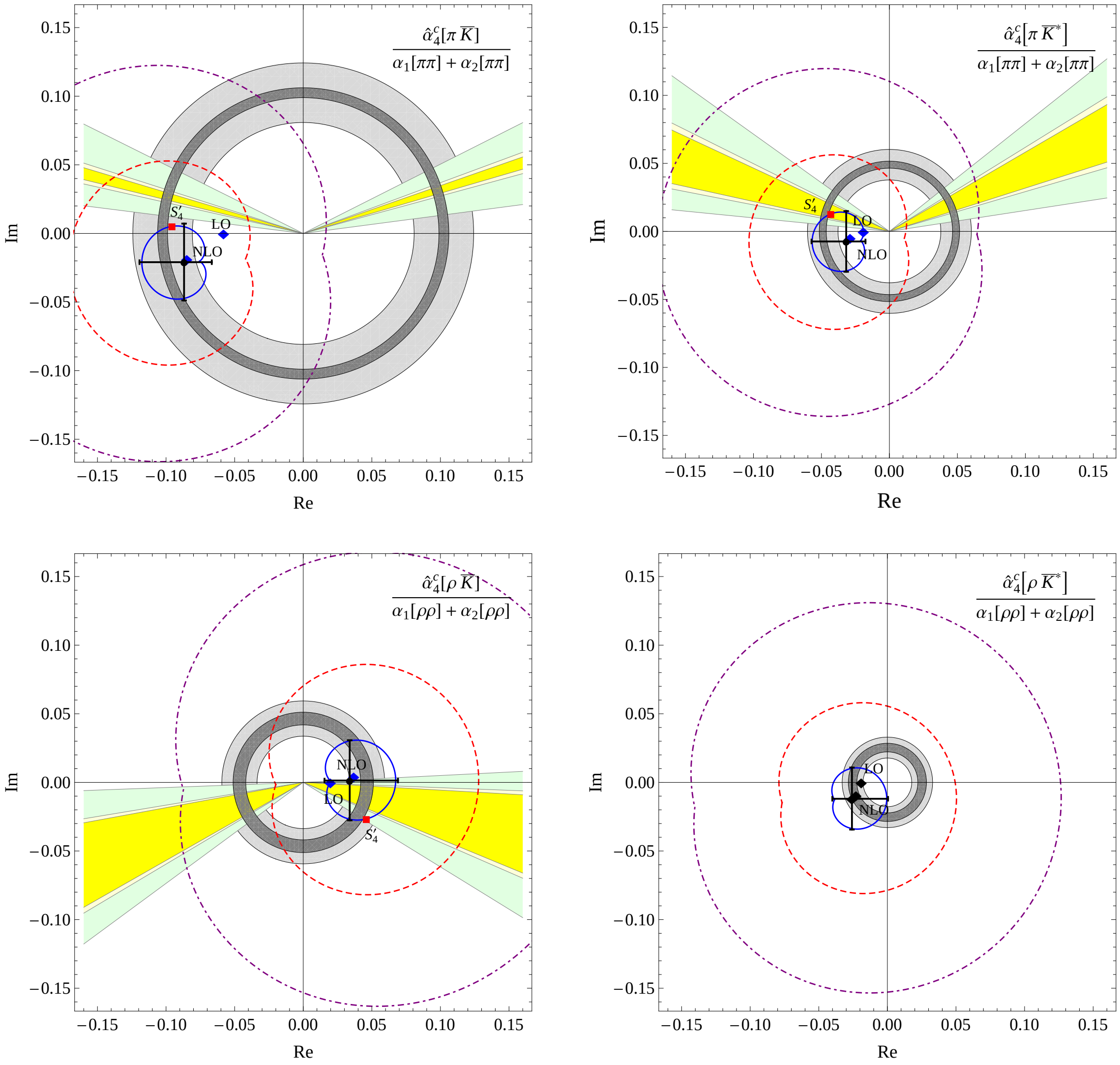

Figure 4: The QCD penguin amplitude $\hat{\alpha}_4^c(M_1M_2)$ for the $PP = \pi K$ final state and its PV, VP, and VV relatives. The VV case refers to the longitudinal polarisation amplitude only. Shown are the theoretical predictions for the ratios $\hat{\alpha}_4^c(M_1M_2)/(\alpha_1(\pi\pi)+\alpha_2(\pi\pi))$ ($\rho\rho$ instead of $\pi\pi$ in the lower row) and a comparison of extractions of the modulus (rings) and phase (wedges) from data. Note there is no data for the CP asymmetry in the rate of the longitudinally polarized ρ^+K^{*-} final state. See text for further explanations.

The theoretical prediction can be compared to data, since the amplitude ratio can be related to CP-averaged decay rates Γ and direct CP asymmetries. We discuss this for the PP case, from which the others can be inferred by obvious replacements. First, to very good approximation [5]

$$\left|\frac{\hat{\alpha}_4^c(\pi\bar{K})}{\alpha_1(\pi\pi)+\alpha_2(\pi\pi)}\right| = \left|\frac{V_{ub}}{V_{cb}}\right| \frac{f_\pi}{f_K} \left[\frac{\Gamma_{\pi^-\bar{K}^0}}{2\Gamma_{\pi^-\pi^0}}\right]^{1/2} , \tag{16}$$

which determines the grey rings around the origin. The darker rings are due to the experimental errors in the branching fractions and the lighter ones include also the uncertainty of $|V_{ub}/V_{cb}|$ (added linearly). To obtain the wedges we define ψ to be the phase of the amplitude ratio shown in the figure, and

$$\mathcal{R} = \frac{\alpha_1(\pi\bar{K}) + \hat{\alpha}_4^u(\pi\bar{K})}{\alpha_1(\pi\pi)+\alpha_2(\pi\pi)} \,. \tag{17}$$

We then find

$$-\sin\psi + \frac{\mathrm{Im}\,\mathcal{R}}{\mathrm{Re}\,\mathcal{R}}\cos\psi = \frac{1}{2\sin\gamma\,\mathrm{Re}\,\mathcal{R}} \left|\frac{V_{cs}}{V_{us}}\right| \frac{f_\pi}{f_K} \frac{\Gamma_{\pi^+K^-}}{\sqrt{2\Gamma_{\pi^-\pi^0}\Gamma_{\pi^-\bar{K}^0}}} A_{\mathrm{CP}}(\pi^+K^-) \,. \tag{18}$$

In previous discussions [5, 9] the experimental error on the observables on the right-hand side and the error on γ combined was large, so that it was justified to assume that $\mathcal{R}$ is real and to neglect the theoretical uncertainty on $\mathrm{Re}\,\mathcal{R}$, which mainly stems from the colour-suppressed tree amplitude $\alpha_2(\pi\pi)$. This is no longer the case. The outer wedge now includes the theoretical uncertainty on $\mathcal{R}$ and γ, which is added linearly to the purely experimental uncertainties (inner wedge). The middle wedge includes the uncertainty from γ only. Note that (18) has two solutions as shown in the figure, but the wedge that does not match the theoretical prediction is excluded by $\Gamma_{\pi^+K^-}/\Gamma_{\pi^-\bar{K}^0} < 1$.

Since the NNLO correction to the amplitude ratio turned out to be small, we can reaffirm the conclusions from [9] in the light of significantly improved data. The different magnitude of the PP penguin amplitude vs. PV, VP and VV is clearly reflected in the data as predicted. There is reasonable quantitative agreement as indicated by the error bars and the small onion-shaped regions corresponding to $\varrho_A = 1$. An annihilation contribution of 0.02 to 0.03 seems to be required, except for the longitudinal VV final states. The red square in the first three plots of Fig. 4 corresponds to the theoretical prediction with $\varrho_A = 1$ and the phase $\phi_A = -55^\circ$ (PP), $\phi_A = -45^\circ$ (PV), $\phi_A = -50^\circ$ (VP) (see [4] for the definition of these quantities), which is similar to the favoured parameter set S4 of [5]. Only the CP asymmetry of the πK final state now appears to require a value larger than $\varrho_A = 1$ for a perfect fit.

Moving to the observables themselves, we show in Table 1 the theoretical predictions for direct CP asymmetries, defined as the rate asymmetry between $\bar{B}$ and B decays, together with the world average of experimental data (last column), compiled from HFAG [26]. We focus on the penguin-dominated $b \to s$ transitions of non-strange B mesons to πK final states and their PV and VP relatives. We also show the CP asymmetry difference

$$\delta(\pi\bar{K}) = A_{\mathrm{CP}}(\pi^0K^-) - A_{\mathrm{CP}}(\pi^+K^-) \tag{19}$$

f	NLO	NNLO	NNLO + LD	Exp
$\pi^-\bar{K}^0$	$0.71^{+0.13+0.21}_{-0.14-0.19}$	$0.77^{+0.14+0.23}_{-0.15-0.22}$	$0.10^{+0.02+1.24}_{-0.02-0.27}$	-1.7 ± 1.6
π^0K^-	$9.42^{+1.77+1.87}_{-1.76-1.88}$	$10.18^{+1.91+2.03}_{-1.90-2.62}$	$-1.17^{+0.22+20.00}_{-0.22-6.62}$	4.0 ± 2.1
π^+K^-	$7.25^{+1.36+2.13}_{-1.36-2.58}$	$8.08^{+1.52+2.52}_{-1.51-2.65}$	$-3.23^{+0.61+19.17}_{-0.61-3.36}$	-8.2 ± 0.6
$\pi^0\bar{K}^0$	$-4.27^{+0.83+1.48}_{-0.77-2.23}$	$-4.33^{+0.84+3.29}_{-0.78-2.32}$	$-1.41^{+0.27+5.54}_{-0.25-6.10}$	1 ± 10
$\delta(\pi\bar{K})$	$2.17^{+0.40+1.39}_{-0.40-0.74}$	$2.10^{+0.39+1.40}_{-0.39-2.86}$	$2.07^{+0.39+2.76}_{-0.39-4.55}$	12.2 ± 2.2
$\Delta(\pi\bar{K})$	$-1.15^{+0.21+0.55}_{-0.22-0.84}$	$-0.88^{+0.16+1.31}_{-0.17-0.91}$	$-0.48^{+0.09+1.09}_{-0.09-1.15}$	-14 ± 11
$\pi^-\bar{K}^{*0}$	$1.36^{+0.25+0.60}_{-0.26-0.47}$	$1.49^{+0.27+0.69}_{-0.29-0.56}$	$0.27^{+0.05+3.18}_{-0.05-0.67}$	-3.8 ± 4.2
π^0K^{*-}	$13.85^{+2.40+5.84}_{-2.70-5.86}$	$18.16^{+3.11+7.79}_{-3.52-10.57}$	$-15.81^{+3.01+69.35}_{-2.83-15.39}$	-6 ± 24
π^+K^{*-}	$11.18^{+2.00+9.75}_{-2.15-10.62}$	$19.70^{+3.37+10.54}_{-3.80-11.42}$	$-23.07^{+4.35+86.20}_{-4.05-20.64}$	-23 ± 6
$\pi^0\bar{K}^{*0}$	$-17.23^{+3.33+7.59}_{-3.00-12.57}$	$-15.11^{+2.93+12.34}_{-2.65-10.64}$	$2.16^{+0.39+17.53}_{-0.42-36.80}$	-15 ± 13
$\delta(\pi\bar{K}^*)$	$2.68^{+0.72+5.44}_{-0.67-4.30}$	$-1.54^{+0.45+4.60}_{-0.58-9.19}$	$7.26^{+1.21+12.78}_{-1.34-20.65}$	17 ± 25
$\Delta(\pi\bar{K}^*)$	$-7.18^{+1.38+3.38}_{-1.28-5.35}$	$-3.45^{+0.67+9.48}_{-0.59-4.95}$	$-1.02^{+0.19+4.32}_{-0.18-7.86}$	-5 ± 45
$\rho^-\bar{K}^0$	$0.38^{+0.07+0.16}_{-0.07-0.27}$	$0.22^{+0.04+0.19}_{-0.04-0.17}$	$0.30^{+0.06+2.28}_{-0.06-2.39}$	-12 ± 17
ρ^0K^-	$-19.31^{+3.42+13.95}_{-3.61-8.96}$	$-4.17^{+0.75+19.26}_{-0.80-19.52}$	$43.73^{+7.07+44.00}_{-7.62-137.77}$	37 ± 11
ρ^+K^-	$-5.13^{+0.95+6.38}_{-0.97-4.02}$	$1.50^{+0.29+8.69}_{-0.27-10.36}$	$25.93^{+4.43+25.40}_{-4.90-75.63}$	20 ± 11
$\rho^0\bar{K}^0$	$8.63^{+1.59+2.31}_{-1.65-1.69}$	$8.99^{+1.66+3.60}_{-1.71-7.44}$	$-0.42^{+0.08+19.49}_{-0.08-8.78}$	6 ± 20
$\delta(\rho\bar{K})$	$-14.17^{+2.80+7.98}_{-2.96-5.39}$	$-5.67^{+0.96+10.86}_{-1.01-9.79}$	$17.80^{+3.15+19.51}_{-3.01-62.44}$	17 ± 16
$\Delta(\rho\bar{K})$	$-8.75^{+1.62+4.78}_{-1.66-6.48}$	$-10.84^{+1.98+11.67}_{-2.09-9.09}$	$-2.43^{+0.46+4.60}_{-0.42-19.43}$	-37 ± 37

Table 1: Direct CP asymmetries in percent for the πK, πK^*, and ρK final states. The theoretical errors shown correspond to the uncertainties due to the CKM and hadronic parameters, respectively. The errors on the experimental values of δ and Δ are computed from those of the individual observables appearing in (20) ignoring possible correlations.

and the asymmetry "sum rule"

$$\Delta(\pi\bar{K}) = A_{\rm CP}(\pi^+K^-) + \frac{\Gamma_{\pi^-\bar{K}^0}}{\Gamma_{\pi^+K^-}}\,A_{\rm CP}(\pi^-\bar{K}^0) - \frac{2\Gamma_{\pi^0K^-}}{\Gamma_{\pi^+K^-}}\,A_{\rm CP}(\pi^0K^-) - \frac{2\Gamma_{\pi^0\bar{K}^0}}{\Gamma_{\pi^+K^-}}\,A_{\rm CP}(\pi^0\bar{K}^0)\,. \tag{20}$$

The latter quantity is expected to be small [27], since the leading CP-violating interference of QCD penguin and tree amplitudes cancels out in the sum. In order to focus on the effect of the new NNLO correction on the perturbatively calculable short-distance part of the CP asymmetry, the columns labelled "NLO" and "NNLO" give the respective results, when the long-distance, power-suppressed terms are set to zero. This means that we set β_3^p to zero, as well as power-suppressed spectator-scattering terms. However, we keep the short-distance dominated, but power-suppressed scalar penguin contributions. The column labelled "NNLO+LD" adds the previously neglected terms back. The main effect is from weak annihilation, for which we adopt the S4-like scenario (S_4') marked by the red square in Fig. 4.

Focusing first on the "NLO" and "NNLO" results, we note that for the PP final states the change is minor, since, as discussed above, a_4^c represents only part of the short-distance penguin amplitude. The situation is different for the πK^* final states where the a_6^c contribution is small, and for the ρK final states where due to the opposite sign of a_4^c and a_6^c a cancellation occurs. In these cases, we observe a large modification for the π^0K^{*-}, π^+K^{*-} and the corresponding ρK final states, for which the CP asymmetry arises predominantly from the imaginary part of $\hat{\alpha}_4^c/\alpha_1$. These modifications are a reflection of the sizable corrections seen in Fig. 2. The effect is much less pronounced in the remaining modes, where the asymmetry is due to interference with $\hat{\alpha}_4^u$ (in case of $\pi^-\bar{K}^{*0}$, $\rho^-\bar{K}^0$) or α_2 (in case of $\pi^0\bar{K}^{*0}$, $\rho^0\bar{K}^0$), and the effect of the NNLO correction cancels to a certain extent in the ratio of interfering amplitudes. Despite these large modifications of some of the PV and VP modes' asymmetries, the long-distance annihilation contribution is always more important numerically, and usually required to obtain a satisfactory description of the data. The modelling of the long-distance contribution also determines the final theoretical uncertainty, which can become very large. Given that the short-distance contribution is now known to NNLO and given the large amount of experimental data, it becomes imperative to better determine the annihilation amplitude, presumably through fits to data.

5 Conclusion

The computation of direct CP asymmetries in charmless B decays at next-to-next-to-leading order in QCD has been a long-standing issue. The long- and short-distance contributions can in principle be of the same order and a NNLO calculation is required to ascertain the perturbative part. In this paper we computed the two-loop contributions of the current-current operators $Q_{1,2}^p$ to the QCD penguin amplitude, which are expected to constitute the dominant contribution, at least to the imaginary part, which is required for observing CP violation. We find a sizable correction to the short-distance part of the direct CP asymmetry, the effect of which is, however, tempered by power-suppressed short- and long-distance terms. Our preliminary conclusion is that the NNLO correction does not help resolving the πK CP asymmetry puzzle, nor does it render the poorly known annihilation terms redundant. The final analysis should, however, include the penguin operator matrix elements, as well as the one from the chromomagnetic operator considered in [14]. The corresponding calculations are in progress.

Acknowledgements

This work was supported in part by the NNSFC of China under contract Nos. 11005032 and 11435003 (XL), by DFG Forschergruppe FOR 1873 “Quark Flavour Physics and Effective Field Theories” (TH) and by the DFG Sonderforschungsbereich/Transregio 9 “Computergestützte Theoretische Teilchenphysik” (MB). GB gratefully acknowledges the support of a University Research Fellowship by the Royal Society. XL is also supported in part by the SRF for ROCS, SEM, by the Open Project Program of SKLTP, ITP, CAS (No. Y4KF081CJ1), and by the self-determined research funds of CCNU from the colleges' basic research and operation of MOE (CCNU15A02037). MB and XL acknowledge the hospitality of the Munich Institute for Astro- and Particle Physics (MIAPP) of the DFG cluster of excellence “Origin and Structure of the Universe”, where this work was finalized.

References

[1] D. Zeppenfeld, Z. Phys. C **8** (1981) 77.

[2] M. Beneke, G. Buchalla, M. Neubert and C. T. Sachrajda, Phys. Rev. Lett. **83** (1999) 1914 [hep-ph/9905312].

[3] M. Beneke, G. Buchalla, M. Neubert and C. T. Sachrajda, Nucl. Phys. B **591** (2000) 313 [hep-ph/0006124].

[4] M. Beneke, G. Buchalla, M. Neubert and C. T. Sachrajda, Nucl. Phys. B **606** (2001) 245 [hep-ph/0104110].

[5] M. Beneke and M. Neubert, Nucl. Phys. B **675** (2003) 333 [hep-ph/0308039].

[6] M. Beneke and S. Jäger, Nucl. Phys. B **751** (2006) 160 [hep-ph/0512351].

[7] N. Kivel, JHEP **0705** (2007) 019 [hep-ph/0608291].

[8] V. Pilipp, Nucl. Phys. B **794** (2008) 154, arXiv:0709.3214 [hep-ph].

[9] M. Beneke and S. Jäger, Nucl. Phys. B **768** (2007) 51 [hep-ph/0610322].

[10] A. Jain, I. Z. Rothstein and I. W. Stewart, arXiv:0706.3399 [hep-ph].

[11] G. Bell, Nucl. Phys. B **795** (2008) 1, arXiv:0705.3127 [hep-ph].

[12] G. Bell, Nucl. Phys. B **822** (2009) 172, arXiv:0902.1915 [hep-ph].

[13] M. Beneke, T. Huber and X. Q. Li, Nucl. Phys. B **832**, 109 (2010), arXiv:0911.3655 [hep-ph].

[14] C. S. Kim and Y. W. Yoon, JHEP **1111** (2011) 003, arXiv:1107.1601 [hep-ph].

[15] G. Bell and T. Huber, JHEP **1412** (2014) 129, arXiv:1410.2804 [hep-ph].

[16] K. G. Chetyrkin, M. Misiak and M. Münz, Nucl. Phys. B **520** (1998) 279 [hep-ph/9711280].

[17] M. Gorbahn and U. Haisch, Nucl. Phys. B **713** (2005) 291 [hep-ph/0411071].

[18] G. Passarino and M. J. G. Veltman, Nucl. Phys. B **160** (1979) 151.

[19] F. V. Tkachov, Phys. Lett. B **100** (1981) 65.

[20] K. G. Chetyrkin and F. V. Tkachov, Nucl. Phys. B **192** (1981) 159.

[21] S. Laporta and E. Remiddi, Phys. Lett. B **379** (1996) 283 [hep-ph/9602417].

[22] S. Laporta, Int. J. Mod. Phys. A **15** (2000) 5087 [hep-ph/0102033].

[23] C. Anastasiou and A. Lazopoulos, JHEP **0407** (2004) 046 [hep-ph/0404258].

[24] J. M. Henn, Phys. Rev. Lett. **110** (2013) 251601, arXiv:1304.1806 [hep-th].

[25] G. Buchalla, A. J. Buras and M. E. Lautenbacher, Rev. Mod. Phys. **68** (1996) 1125 [hep-ph/9512380].

[26] Y. Amhis *et al.* [Heavy Flavor Averaging Group Collaboration], arXiv:1412.7515 [hep-ex], and update at http://www.slac.stanford.edu/xorg/hfag/.

[27] M. Gronau, Phys. Lett. B **627** (2005) 82 [hep-ph/0508047].